British Journal of Pharmacology

DOI:10.1111/bph.13077
www.brjpharmacol.org

RESEARCH PAPER

9-Phenanthrol inhibits recombinant and arterial myocyte TMEM16A channels

Sarah K Burris, Qian Wang, Simon Bulley, Zachary P Neeb and Jonathan H Jaggar

Department of Physiology, University of Tennessee Health Science Center, Memphis, TN, USA

Correspondence
Jonathan H Jaggar, Department of Physiology, University of Tennessee Health Science Center, Memphis, TN 38163, USA.
E-mail: jjaggar@uthsc.edu

Received
7 December 2013
Revised
19 December 2014
Accepted
23 December 2014

BACKGROUND AND PURPOSE

In arterial smooth muscle cells (myocytes), intravascular pressure stimulates membrane depolarization and vasoconstriction (the myogenic response). Ion channels proposed to mediate pressure-induced depolarization include several transient receptor potential (TRP) channels, including TRPM4, and transmembrane protein 16A (TMEM16A), a Ca^{2+}-activated Cl^- channel (CaCC). 9-Phenanthrol, a putative selective TRPM4 channel inhibitor, abolishes myogenic tone in cerebral arteries, suggesting that either TRPM4 is essential for pressure-induced depolarization, upstream of activation of other ion channels or that 9-phenanthrol is non-selective. Here, we tested the hypothesis that 9-phenanthrol is also a TMEM16A channel blocker, an ion channel for which few inhibitors have been identified.

EXPERIMENTAL APPROACH

Patch clamp electrophysiology was used to measure rat cerebral artery myocyte and human recombinant TMEM16A (rTMEM16A) currents or currents generated by recombinant bestrophin-1, another Ca^{2+}-activated Cl^- channel, expressed in HEK293 cells.

KEY RESULTS

9-Phenanthrol blocked myocyte TMEM16A currents activated by either intracellular Ca^{2+} or E_{act}, a TMEM16A channel activator. In contrast, 9-phenanthrol did not alter recombinant bestrophin-1 currents. 9-Phenanthrol reduced arterial myocyte TMEM16A currents with an IC_{50} of ~12 μM. Cell-attached patch recordings indicated that 9-phenanthrol reduced single rTMEM16A channel open probability and mean open time, and increased mean closed time without affecting the amplitude.

CONCLUSIONS AND IMPLICATIONS

These data identify 9-phenanthrol as a novel TMEM16A channel blocker and provide an explanation for the previous observation that 9-phenanthrol abolishes myogenic tone when both TRPM4 and TMEM16A channels contribute to this response. 9-Phenanthrol may be a promising candidate from which to develop TMEM16A channel-specific inhibitors.

Abbreviations

E_{act}, small-molecule TMEM16A activator; TMEM16A, transmembrane protein 16A; TRPM4, transient receptor potential melastatin 4

Tables of Links

TARGETS	
Ca_v channels	TRPC6
K_{ir} channels	TRPM2
K_v channels	TRPM4
Large conductance Ca^{2+}-activated K^+ (BK) channels	TRPM5
TMEM16A	TRPP1
TRPC3	

LIGANDS	
9-Phenanthrol	DPC
ATP	Niflumic acid
Bestrophin-3	NPPB
DIDS	

These Tables list key protein targets and ligands in this article which are hyperlinked to corresponding entries in http://www.guidetopharmacology.org, the common portal for data from the IUPHAR/BPS Guide to PHARMACOLOGY (Pawson *et al.*, 2014) and are permanently archived in the Concise Guide to PHARMACOLOGY 2013/14 (Alexander *et al.*, 2013).

Introduction

Intravascular pressure stimulates vasoconstriction in resistance-size arteries via a smooth muscle-dependent reaction termed the myogenic response (Meininger and Davis, 1992; Hill *et al.*, 2001). This functional signalling pathway is considered to be particularly significant in the vasculature of certain organs, including the brain and kidney. The myogenic response contributes to the maintenance of blood flow over a range of intravascular pressures, regulates regional organ blood flow, and provides a baseline from which vasoconstrictors and vasodilators can modulate contractility (Meininger and Davis, 1992). Research over the past two decades has focused on identifying mechanisms that underlie the myogenic response. Still uncertain and subject to investigation are the pressure mechanosensing mechanisms present in arterial smooth muscle cells that mediate this vasoconstriction.

An elevation in intravascular pressure stimulates arterial depolarization, which activates smooth muscle cell voltage-dependent calcium (Ca_v) channels (Nelson *et al.*, 1990). This leads to Ca^{2+} influx, an elevation in intracellular Ca^{2+} concentration, and vasoconstriction (Nelson *et al.*, 1990). Several ion channels have been proposed to contribute to pressure-induced depolarization in arterial smooth muscle cells (Nelson *et al.*, 1990; Jackson, 2000). These include non-selective transient receptor potential canonical 6 (TRPC6), melastatin 4 (TRPM4) and polycystin 2 (TRPP2) channels (Brayden *et al.*, 2008; Earley and Brayden, 2010; Guibert *et al.*, 2011). Transmembrane protein 16A (TMEM16A) Ca^{2+}-activated Cl^- (CaCC) channels are expressed in arterial myocytes of several different vascular beds and also contribute to pressure-induced membrane depolarization and vasoconstriction in cerebral arteries (Namkung *et al.*, 2011; Bulley *et al.*, 2012; Huang *et al.*, 2012). Selective pharmacological modulators of TRPC6, TRPM4, TRPP2 and TMEM16A channels are rare. Functional evidence supporting the involvement of these ion channels in the myogenic response has primarily been obtained by inducing partial protein knockdown (Dietrich *et al.*, 2005; Bulley *et al.*, 2012; Gonzales and Earley, 2012; Narayanan *et al.*, 2013). Pharmacological responses to 9-hydroxyphenanthrene (9-phenanthrol), a benzoquinolizinium derivative and putative selective TRPM4 channel inhibitor, have been studied in cerebral arteries (Gonzales *et al.*, 2010). 9-Phenanthrol essentially abolished pressure-induced membrane depolarization and vasoconstriction (Gonzales *et al.*, 2010). These data suggested that TRPM4 channels are either the only, or principal, ion channel mediating pressure-induced depolarization or that TRPM4 activation is upstream or downstream of stimulation of TRPC6, TRPP2 and TMEM16A channels. An additional possibility is that 9-phenanthrol is non-selective and blocks other ion channels that mediate pressure-induced membrane depolarization and vasoconstriction. At first, this hypothesis does not appear to have significant merit as 9-phenanthrol has been demonstrated to not modulate currents mediated by TRPM5, TRPC3, TRPC6, TRPM7, large-conductance Ca^{2+}-activated K^+ (BK), inward-rectifier K^+(K_{ir}), voltage-dependent K^+ (K_v) and voltage-dependent Ca^{2+} (Ca_v) channels (Grand *et al.*, 2008; Gonzales *et al.*, 2010; Kim *et al.*, 2011). However, whether 9-phenanthrol regulates TMEM16A channels has not been investigated. Given that few inhibitors of TMEM16A channels have been identified, this hypothesis is worth testing.

Using patch clamp electrophysiology, we demonstrated that 9-phenanthrol inhibits both cerebral artery myocyte and recombinant TMEM16A (rTMEM16A)-mediated currents. 9-Phenanthrol also blocked TMEM16A currents that were activated by either intracellular Ca^{2+} or E_{act}, a direct channel activator. In contrast, 9-phenanthrol did not alter currents generated by recombinant bestrophin-1, mediated by another Ca^{2+}-activated Cl^- channel. Single channel recordings indicated that 9-phenanthrol reduces TMEM16A channel open probability by decreasing mean open time and increasing mean closed time. Taken together, we demonstrated that 9-phenanthrol inhibits cerebral artery myocyte and recombinant TMEM16A channels by altering channel gating. These data not only identify 9-phenanthrol as a novel TMEM16A channel blocker, but also provide an explanation for the previous observation that 9-phenanthrol abolishes myogenic tone when both TRPM4 and TMEM16A channels contribute to this response.

Methods

Animals and myocyte preparation

Animal protocols were reviewed and approved by the Animal Care and Use Committee at the University of Tennessee

Health Science Center. Male Sprague-Dawley rats (6–8 weeks) were killed by injection of an overdose of sodium pentobarbital (150 mg·kg^{-1}, i.p.). Cerebral arteries were isolated from a total of 30 rats for this study. The brain was removed and placed in physiological saline solution composed of (in mmol·L^{-1}): 112 NaCl, 4.8 KCl, 24 $NaHCO_3$, 1.8 $CaCl_2$, 1.2 $MgSO_4$, 1.2 KH_2PO_4, and 10 glucose that was gassed with 21% O_2 – 5% CO_2 – 74% N_2 to pH 7.4. Resistance-size (~200 μm diameter) posterior cerebral and cerebellar arteries were dissected from the brain and used for experimentation. Myocytes were isolated from cerebral arteries as previously described (Jaggar, 2001). All studies involving animals are reported in accordance with the ARRIVE guidelines for reporting experiments involving animals (Kilkenny *et al.*, 2010; McGrath *et al.*, 2010).

HEK cell culture and transfection

HEK293 cells were maintained in DMEM supplemented with 10% FBS and 1% penicillin-streptomycin under standard tissue culture conditions (21% O_2 – 5% CO_2; 37°C). HEK293 cells were transiently transfected with pcDNA3 encoding full-length human TMEM16A (1 μg, rTMEM16A) as previously described (Bulley *et al.*, 2012) or human bestrophin-1 (1 μg), a gift from Dr Criss Hartzell (Emory University). Cells were cotransfected with a vector encoding GFP to permit identification using fluorescence microscopy. Cells were used within 36 h after transfection.

Patch clamp electrophysiology

Membrane currents were recorded using an Axopatch 200B amplifier equipped with a CV 203BU headstage, Digidata 1332A, and Clampex 8 or 9 (Molecular Devices, Sunnyvale, CA, USA). Pipettes were pulled from borosilicate glass, heat polished to 1–3 MΩ, and waxed to reduce capacitance. For cerebral artery myocytes, the pipette solution contained (in mmol·L^{-1}): 126 CsCl, 10 HEPES, 10 glucose, 1 EGTA, 1 Mg-ATP, 0.2 GTP-Na and 40 sucrose, with pH adjusted to 7.2 with CsOH. Free Ca^{2+} (600 nM or 1 μM) and Mg^{2+} (2 μM) were calculated using WebmaxC Standard (http://www.stanford.edu/~cpatton/webmaxcS.htm). The bath solution contained (in mmol·L^{-1}): 126 NMDG-Cl, 10 HEPES, 1.2 $MgCl_2$, 2 $CaCl_2$, 10 glucose and 40 sucrose, with pH adjusted to 7.4 using HCl. In myocytes, whole-cell Ca^{2+}-activated Cl^- currents were measured by applying 1.5 s voltage steps to between –80 and +120 mV in 20 mV increments using an interpulse holding potential of –40 mV. When an intracellular free Ca^{2+} concentration of 600 nM was used, voltage steps were applied between –100 and +100 mV in 20 mV increments. For experiments using E_{act}, the pipette solution contained (in mmol·L^{-1}): 130 CsCl, 10 HEPES, 0.5 EGTA, 1 Mg-ATP and 1 $MgCl_2$, with pH adjusted to 7.2 using CsOH. Free Ca^{2+} was 200 nM and Mg^{2+} was 2 μM. E_{act} was applied via the pipette solution. The bath solution contained (in mmol·L^{-1}): 140 NMDG-Cl, 10 glucose, 10 HEPES, 1 $MgCl_2$ and 1 $CaCl_2$, with pH adjusted to 7.4 using HCl. For E_{act} experiments, whole-cell Cl^- currents were measured by applying 1.5 s voltage steps to between –90 and +110 mV in 20 mV increments using an interpulse holding potential of +10 mV. 9-Phenanthrol was applied via the bath solution. The time course of 9-phenanthrol current inhibition was measured by applying repetitive voltage steps specified in the figure legends. Current density (pA/pF) was calculated by normalizing membrane current to membrane capacitance.

To record rTMEM16A currents in HEK 293 cells, the pipette solution contained (in mmol·L^{-1}): 146 CsCl, 2 $MgCl_2$, 5 EGTA, 10 HEPES, 10 sucrose and 1 μM free Ca^{2+}, with pH adjusted to 7.2 using CsOH. The bath solution contained (in mmol·L^{-1}): 140 NaCl, 5 KCl, 2 $CaCl_2$, 1 $MgCl_2$, 15 glucose and 10 HEPES, with pH adjusted to 7.4 using NaOH. Up to 350 ms voltage steps to between –100 and +100 mV followed by a 150 ms step to –100 mV were applied every 4 s. Currents were filtered at 1 kHz using a low pass Bessel filter and digitized at 4 kHz. rTMEM16A currents were corrected for time-dependent rundown, the mean rate of which was calculated (4.7% min^{-1}) by recording currents subjected to a repetitive ramp protocol between –100 and +100 mV (n = 10).

Recombinant bestrophin-1 currents were recorded in HEK293 cells using a pipette solution containing (in mmol·L^{-1}): 146 CsCl, 2 $MgCl_2$, 5 EGTA, 8 HEPES and 10 sucrose, pH 7.3 with CsOH, with a free Ca^{2+} concentration of 4.5 μM. The bath solution contained (in mmol·L^{-1}): 140 NaCl, 4 KCl, 1 $MgCl_2$, 2 $CaCl_2$, 10 HEPES and 10 glucose, pH 7.3 with NaOH. The currents were measured by applying 500 ms pulses from –100 to +100 mV in 20 mV increments from a holding potential of 0 mV. The currents were filtered at 1 kHz using a low pass Bessel filter and digitized at 4 kHz.

For cell-attached patch measurements, the bath and pipette solutions both contained (in mmol·L^{-1}): 140 NaCl, 5 KCl, 2 $CaCl_2$, 1 $MgCl_2$, 10 HEPES and 15 glucose (pH 7.4, NaOH). Single TMEM16A channel currents were measured at a steady membrane potential of –80 mV.

Statistical analysis

GraphPad Prism software (GraphPad Software, Inc., La Jolla, CA, USA) was used for statistical analyses. Values are expressed as mean ± SEM. Student's *t*-test was used for comparing paired and unpaired data from two populations, and two-way ANOVA with Bonferroni *post hoc* test used for multiple group comparisons. $P < 0.05$ was considered significant. Power analysis was performed on all data where $P > 0.05$ to verify that sample size was sufficient to give a power value >0.8.

Results

Whole-cell TMEM16A currents were isolated and recorded in rat cerebral artery myocytes using experimental conditions that we have previously described (Thomas-Gatewood *et al.*, 2011). TMEM16A currents were activated by including 1 μM free intracellular Ca^{2+} in the pipette solution, which generates a Cl^- current that is primarily due to TMEM16A channels, as previously demonstrated using approaches including anion substitution, elevation of intracellular Ca^{2+} concentration, inhibition by a TMEM16A antibody that blocks recombinant TMEM16A currents, and TMEM16A-specific knockdown using RNAi (Thomas-Gatewood *et al.*, 2011; Bulley *et al.*, 2012). The mean rectification index (I_{80}/I_{-80}) of the current here was 1.15, which is consistent with that previously measured when using the same recording conditions (Figure 1B) (Thomas-Gatewood *et al.*, 2011). 9-Phenanthrol reversibly

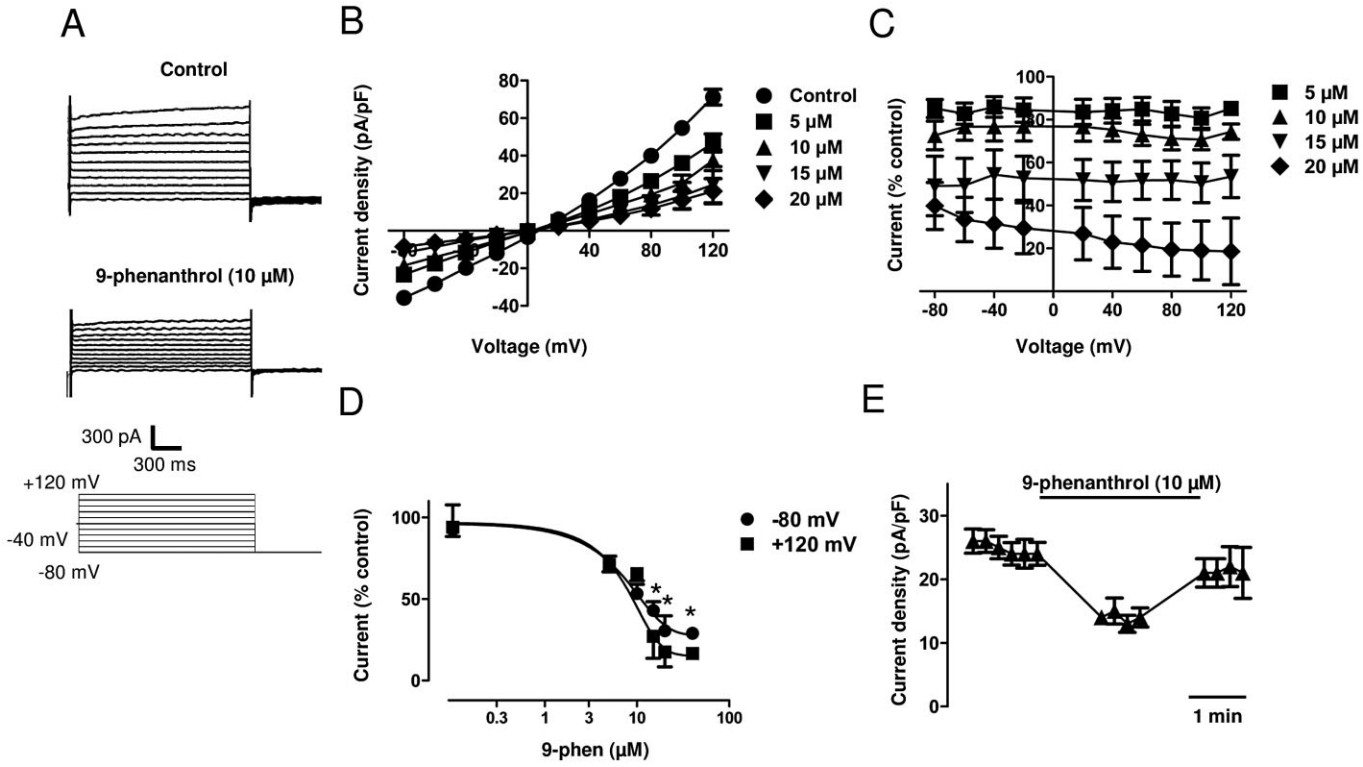

Figure 1

9-Phenanthrol inhibits TMEM16A currents in cerebral artery smooth muscle cells. (A) Examples of whole-cell TMEM16A currents recorded in the absence (control) and presence of 9-phenanthrol (10 μM) in a smooth muscle cell. (B) Mean grouped data for whole-cell currents: control, n = 8; 9-phenanthrol: 5 μM, n = 7; 10 μM, n = 6; 15 μM, n = 5; 20 μM, n = 4. P was < 0.05 when compared with control for: 5 μM at +80, +100, and +120 mV, 10 μM at –80, –60, +60, +80, +100 and +120 mV; 15 μM at –80, –60, –40, +60, +80, +100 and +120 mV; 20 μM at –80, –60, –40, +40, +60, +80, +100 and +120 mV. (C) Mean data illustrating concentration- and voltage-dependence of 9-phenanthrol inhibition determined from tail currents. (D) Concentration-response mediated inhibition of whole-cell TMEM16A currents by 9-phenanthrol at –80 and +120 mV determined from tail currents (same ns as in B, including 0.1 μM, n = 5; 40 μM, n = 4). (E) Mean data displaying current density generated by a 360 ms depolarizations from –40 to +60 mV every 15 s illustrating the time course of 9-phenanthrol (10 μM) inhibition (n = 8) and washout (n = 5). Data points during solution exchange are not shown due to electrical noise in the recordings. *Indicates P < 0.05.

inhibited TMEM16A currents in a concentration-dependent manner (Figure 1A–E). 9-Phenanthrol inhibition was not voltage dependent at concentrations less than 15 μM, being similar at –80 and +120 mV (Figure 1D). In contrast, at concentrations greater than 15 μM, 9-phenanthrol was a more effective inhibitor at positive potentials (Figure 1B and D). Concentration–response curves were fit with a Hill equation yielding IC_{50}s of 12.8 and 11.4 μM at –80 and +120 mV respectively (Figure 1D). Figure 1E illustrates the time course of 9-phenanthrol inhibition of TMEM16A currents demonstrating rapid onset, sustained inhibition and washout. Responses to 9-phenanthrol were also studied when using an intracellular free Ca^{2+} concentration of 600 nM, which generates outwardly rectifying TMEM16A currents (I_{80}/L_{80}, 2.07; Supporting Information Fig. S1). With 600 nM intracellular free Ca^{2+}, 9-phenanthrol (10 μM) inhibited TMEM16A currents to 40.0 ± 3.8% of control at –100 mV and to 43.9 ± 1.4% of control at +100 mV (Supporting Information Fig. S1). These data indicate that 9-phenanthrol inhibits TMEM16A currents with some voltage dependency at higher concentrations in arterial myocytes.

E_{act}, an N-aroylaminothiazole that directly activates TMEM16A channels independently of Ca^{2+}, was used as an alternative mechanism to examine 9-phenanthrol regulation in arterial myocytes (Namkung *et al.*, 2011). In these experiments, the pipette solution contained 200 nM free Ca^{2+}, which generated currents with a mean rectification index (I_{90}/L_{90}) of 4.1 (Figure 2B). Inclusion of E_{act} in the pipette solution stimulated Cl^- currents and reduced the mean rectification index (I_{90}/L_{90}) to 1.32 (Figure 2A and B). 9-Phenanthrol reversibly inhibited E_{act}-activated Cl^- currents in a concentration-dependent manner (Figure 2A–C). For example, at –90 and +90 mV, 9-phenanthrol (10 μM) reduced the mean current density to ~47 and 34% of that in E_{act} alone, respectively. Figure 2C illustrates time-dependent inhibition of E_{act}-stimulated myocyte TMEM16A currents and washout. These data provide additional evidence that 9-phenanthrol blocks TMEM16A currents in arterial myocytes and suggest that inhibition occurs via a Ca^{2+}-independent mechanism.

To further investigate the hypothesis that 9-phenanthrol blocks TMEM16A channels and to investigate mechanisms of block, currents generated by rTMEM16 channels were examined with 1 μM free Ca^{2+} in the pipette solution (Figure 3A–E). 9-Phenanthrol inhibited rTMEM16A currents in a concentration-dependent manner (Figure 3B and C). Concentration–response curves fit with a Hill equation

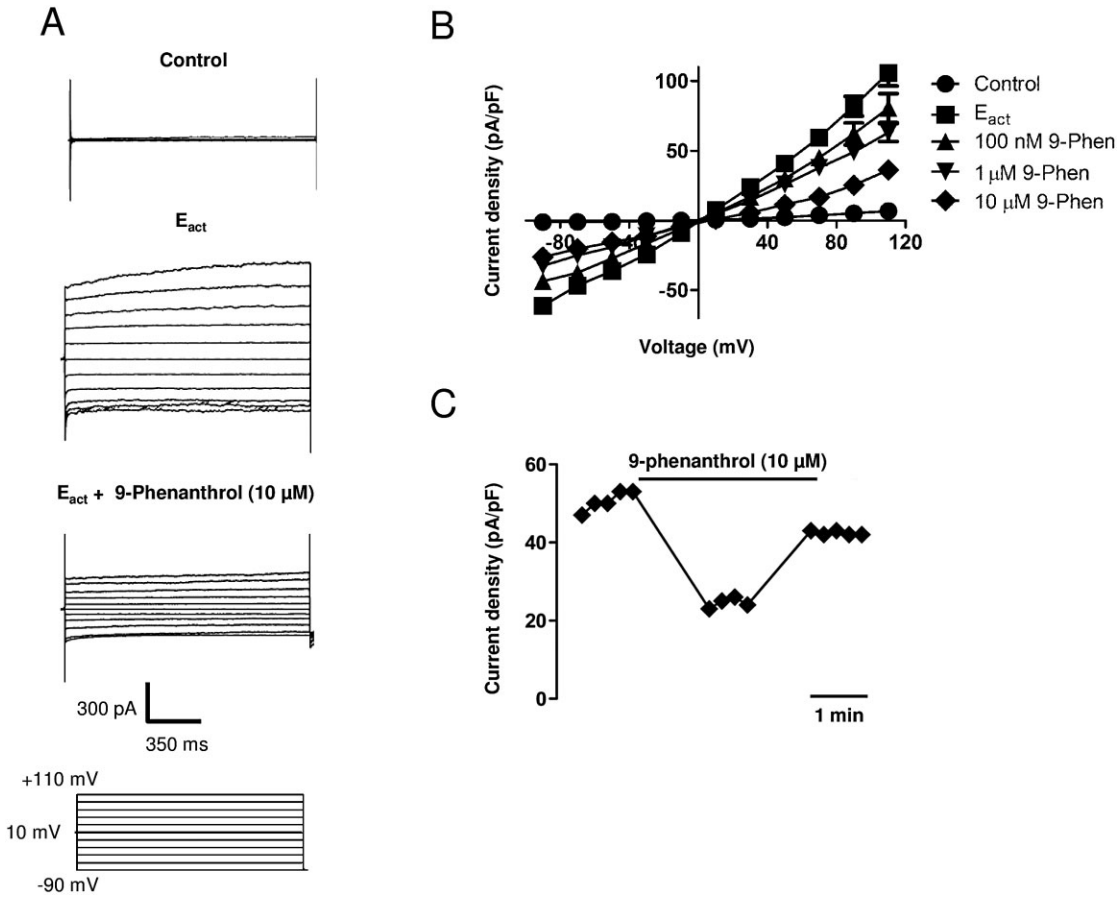

Figure 2

TMEM16A currents activated by E_{act}, a TMEM16A channel activator, are blocked by 9-phenanthrol in arterial smooth muscle cells. (A) Examples of Cl^- current regulation by E_{act} and 9-phenanthrol applied in the presence of E_{act}. E_{act} (10 μM) and E_{act} + 9-phenanthrol (10 μM) recordings are from the same cell. (B) Mean data illustrating concentration-dependent inhibition of E_{act}-activated TMEM16A currents by 9-phenanthrol. $P < 0.05$ when compared with control for: 100 nM at −90, +70, +90 and +110 mV, 1 μM at −90, −70, −50, +70, +90 and +110 mV; 10 μM at −90, −70, −50, +30, +50, +70, +90 and +110 mV. Control, $n = 8$; E_{act} (10 μM), $n = 7$; E_{act} + 100 nM 9-phenanthrol, $n = 7$; E_{act} + 1 μM 9-phenanthrol, $n = 6$; E_{act} + 10 μM 9-phenanthrol, $n = 6$. (C) Mean data displaying current density generated by 360 ms voltage steps from +10 to +70 mV every 15 s illustrating the time course of 9-phenanthrol inhibition and washout. Data points during exchange are not shown due to electrical noise in the recordings.

revealed IC_{50}s of 3.4 μM at −100 mV and 1.8 μM at +100 mV (Figure 3D). Similar to data in arterial myocytes, 9-phenanthrol inhibited TMEM16A more at positive voltages. For example, 10 μM 9-phenanthrol reduced mean rTMEM16A currents ~40 and 60% at −100 and +100 respectively (Figure 3B and C). Figure 3E illustrates the time course of 9-phenanthrol inhibition of rTMEM16A currents demonstrating rapid onset, sustained inhibition and washout.

To investigate the specificity of 9-phenanthrol for TMEM16A channels, regulation of recombinant bestrophin-1, another Ca^{2+}-activated Cl^- channel, was examined. HEK293 cells were transfected with bestrophin-1 and whole-cell currents were recorded using a pipette solution containing an intracellular free Ca^{2+} concentration of 4.5 μM. Recombinant bestrophin-1-transfected cells generated Cl^- currents phenotypically similar to those previously described (Figure 4A and B) (Fischmeister and Hartzell, 2005). The current density of bestrophin-1-transfected cells was ~5.7- and 17.0-fold larger at +100 and −100 mV, respectively, than those in mock-transfected cells (Figure 4B). 9-Phenanthrol did not alter recombinant bestrophin-1 currents when applied at concentrations between 100 nM and 100 μM (Figure 4A and B). Taken together, these data indicate that 9-phenanthrol is specific for TMEM16A over bestrophin-1, and therefore is not a non-specific Ca^{2+}-activated Cl^- channel inhibitor.

Mechanisms by which 9-phenanthrol inhibits TMEM16A channels were examined. Single channels were recorded at −80 mV in cell-attached patches of mock-transfected and rTMEM16A-transfected HEK293 cells. In mock HEK293 cells, channel activity was rare and unaffected by 9-phenanthrol (Figure 5A, Supporting Information Fig. S2). In cells expressing rTMEM16A, single channel openings were observed that were identified as rTMEM16A based on a mean single channel amplitude (0.40 ± 0.06, Figure 5A and B) matching that previously described (Bulley *et al.*, 2012; Davis *et al.*, 2013). 9-Phenanthrol reduced mean single TMEM16A channel open probability (P_o) from ~0.49 to 0.20, or by 59% (Figure 5A, C,

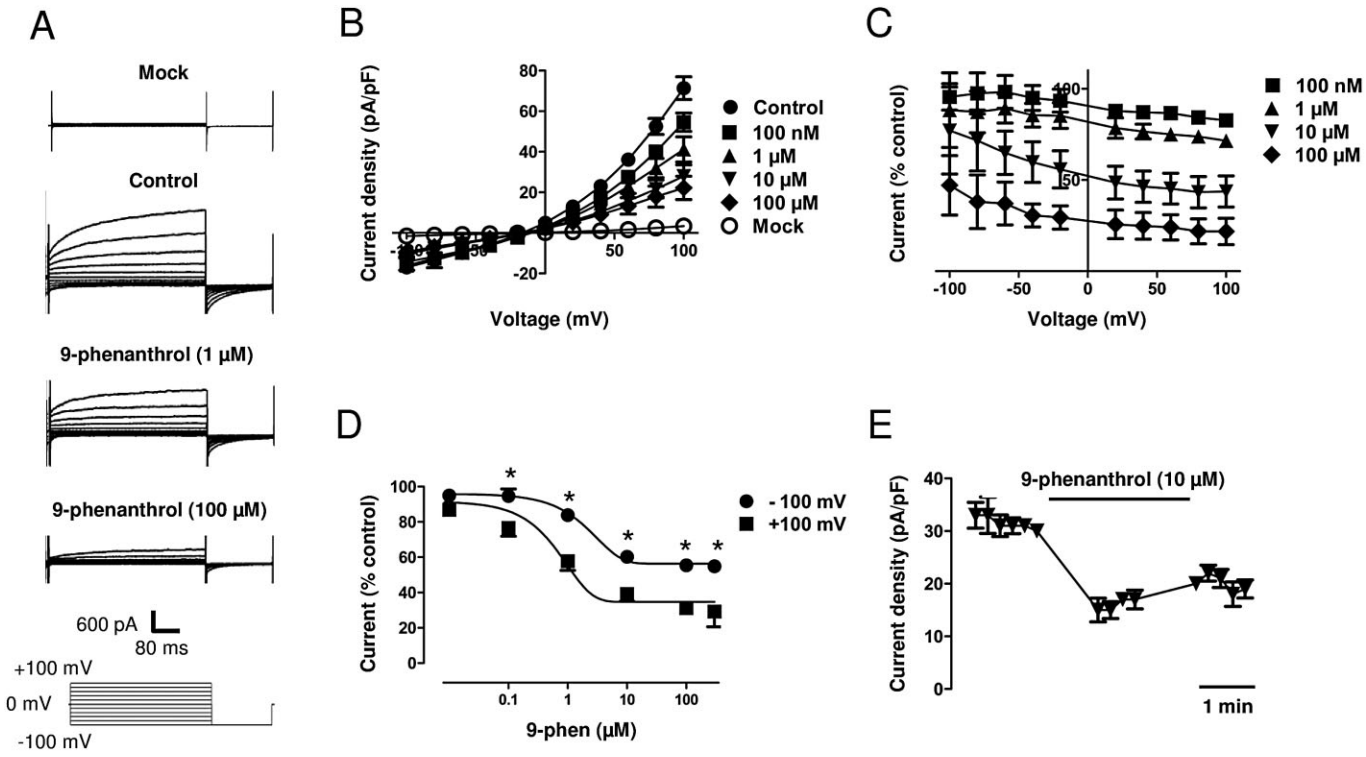

Figure 3

Recombinant TMEM16A currents in HEK 293 cells are inhibited by 9-phenanthrol. (A) Original recordings of rTMEM16A currents and inhibition by 9-phenanthrol in HEK293 cells. (B) Mean data for whole-cell currents: control, $n = 17$; 100 nM 9-phenanthrol, $n = 15$; 1 μM 9-phenanthrol, $n = 14$; 10 μM 9-phenanthrol, $n = 11$; 100 μM 9-phenanthrol, $n = 11$. (C) Mean data illustrating concentration- and voltage-dependence of 9-phenanthrol rTMEM16A current inhibition determined from tail currents. (D) Concentration-dependent inhibition of rTMEM16A currents at –100 and +100 mV (same *n*s as in B, including 0.1 μM, $n = 15$; 300 μM, $n = 7$). (E) Mean data displaying current density generated by repetitive steps from 0 to +60 mV illustrating 9-phenanthrol inhibition ($n = 6$) and washout ($n = 5$). Data points during solution exchange are not shown due to electrical noise in the recordings. *Indicates $P < 0.05$ when compared with control currents.

D, E). 9-Phenanthrol reduced channel mean open time and increased mean closed time (Figure 5F and G). In contrast, 9-phenanthrol did not alter TMEM16A single channel amplitude (Figure 5B). These data indicate that 9-phenanthrol inhibits TMEM16A currents by reducing channel open time and increasing closed time, which reduces P_o.

Discussion and conclusions

Here, we showed that 9-phenanthrol, a putative selective TRPM4 channel inhibitor, blocks cerebral artery smooth muscle cell and recombinant TMEM16A channels. 9-Phenanthrol did not alter recombinant bestrophin-1 currents, indicating that 9-phenanthrol exhibits selectivity for TMEM16A channels. 9-Phenanthrol reduced TMEM16A channel mean open time and increased mean closed time. In contrast, 9-phenanthrol did not alter single channel amplitude, indicating that 9-phenanthrol modifies channel gating and does not appear to be a pore blocker. These data rationalize how 9-phenanthrol can abolish myogenic tone, when TRPM4 and TMEM16A channels have both been described to contribute to pressure-induced depolarization and myogenic tone development. Our results also describe a novel TMEM16A channel inhibitor from which other more selective TMEM16A channel inhibitors could be developed. These findings are significant as TMEM16A channel inhibitors that could be used to treat disease are rare. It is also possible that combined inhibition of TRPM4 and TMEM16A by 9-phenanthrol or molecular derivatives may be therapeutically useful.

9-Phenanthrol was initially discovered as an inhibitor of TRPM4, but not TRPM5, currents (Grand *et al.*, 2008). Subsequent studies indicated that 9-phenanthrol failed to modify currents generated by other TRP channels, including TRPC3, TRPC6 and TRPM7 (Gonzales *et al.*, 2010; Kim *et al.*, 2011). 9-Phenanthrol also does not regulate large-conductance Ca^{2+}-activated K^+, inward-rectifier K^+, voltage-dependent K^+ and voltage-dependent Ca^{2+} currents in cerebral artery myocytes (Gonzales *et al.*, 2010). Several findings here indicate that 9-phenanthrol blocks arterial myocyte TMEM16A currents. These include the observation that 9-phenanthrol inhibited cerebral artery myocyte Ca^{2+}-activated Cl^- currents that occur due to TMEM16A channels (Bulley *et al.*, 2012), myocyte Cl^- currents activated by E_{act}, a TMEM16A channel activator, whole-cell rTMEM16A currents, with similar micromolar IC_{50}s for arterial myocyte and rTMEM16A currents, and single rTMEM16A channels. It is unlikely that the 9-phenanthrol-

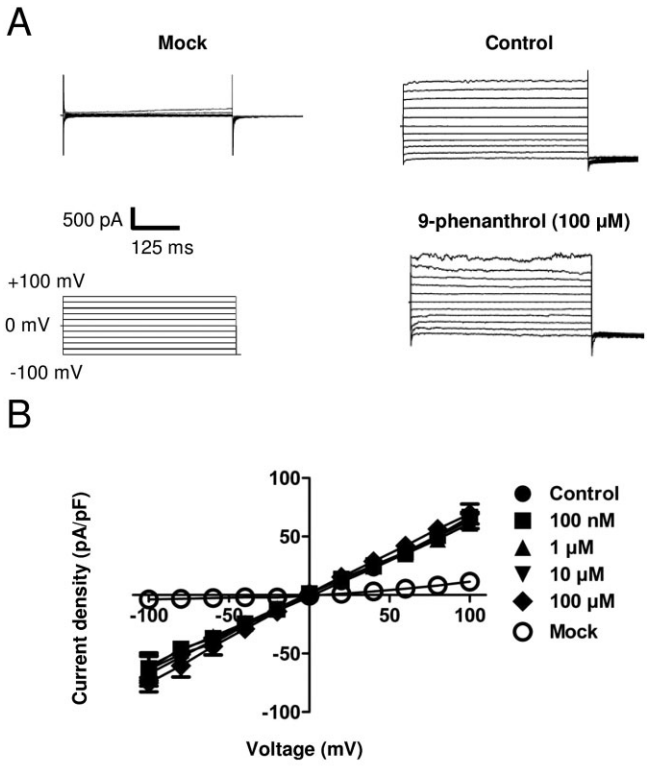

Figure 4

9-Phenanthrol does not modulate recombinant bestrophin-1 currents in HEK 293 cells. (A) Representative recordings illustrating that bestrophin-1 expression generates whole-cell Cl^- currents in HEK293 cells, and that these currents are unaffected by application of 9-phenanthrol (100 µM). (B) Mean data: control, n = 10. 9-Phenanthrol: 100 nM, n = 10; 1 µM, n = 10; 10 µM, n = 6; 100 µM, n = 5; mock, n = 5.

inhibited currents recorded here in arterial myocytes occur due to TRPM4 channels. Firstly, bath and pipette solutions contained NMDG and Cs^+, which are not optimal for measuring non-selective cation currents. Secondly, TRPM4 channels are activated by high (>10 µM) intracellular Ca^{2+} concentrations (Gonzales and Earley, 2012). The pipette solution in our experiments contained 200 nM free Ca^{2+} for E_{act} experiments and 1 µM free Ca^{2+} for Ca^{2+}-activation experiments, which is insufficient for TRPM4 activation. Thirdly, the pipette solution contained 1 mM ATP, a TRPM4 inhibitor (Nilius *et al.*, 2004). Fourthly, TRPM4 undergoes fast desensitization, leading to loss of activity within 2 min following exposure to high Ca^{2+} necessary for activation (Earley *et al.*, 2004; 2007; Launay *et al.*, 2004; Nilius *et al.*, 2004; 2006). In our experiments, TMEM16A currents were activated for as long as patches could be maintained (~15 min). Finally, and more importantly, 9-phenanthrol blocked rTMEM16A currents. In a recent study it was demonstrated that HEK293 cells generate large endogenous TRPM4 currents with low Ca^{2+} sensitivity (EC_{50} of ~61 µM) that can be recorded in the absence of intracellular ATP (Amarouch *et al.*, 2013). These endogenous currents were reduced to 17% of control by 100 µM ATP (Amarouch *et al.*, 2013). Here, we measured small endogenous currents in mock-transfected cells using 1 µM intracellular free Ca^{2+} concentration and a pipette solution containing 1 mM ATP, which would essentially abolish the previously described endogenous TRPM4 currents. Our data indicate that the currents recorded in cells transfected with a construct encoding TMEM16A occur due to TMEM16A channels. To our knowledge, our data are the first to demonstrate that 9-phenanthrol blocks an ion channel other than TRPM4. Interestingly, the IC_{50s} for 9-phenanthrol inhibition of cerebral artery myocyte TMEM16A (12.8 µM at –80 mV) and TRPM4 (10.6 µM at –70 mV) currents are similar (Gonzales *et al.*, 2010). Whether 9-phenanthrol inhibits TMEM16A and TRPM4 channels by a similar mechanism remains to be determined, although this would be surprising given the highly dissimilar molecular structure of these channels.

Several highly non-selective Ca^{2+}-activated Cl^- channel blockers, including niflumic acid, DIDS, NPPB and DPC, inhibit TMEM16A channels (Schroeder *et al.*, 2008). More recent TMEM16A inhibitors have been described, including dichlorophen (IC_{50} 5.49 µM), benzbromarone (IC_{50} 9.97 µM), hexachlorophene (IC_{50} 10 µM) and T16Ainh-A01 (IC_{50} 10 µM) (Huang *et al.*, 2012; Mazzone *et al.*, 2012). These second-generation inhibitors typically block TMEM16A channels at lower concentrations than the highly non-selective blockers, although selectivity has yet to be established. Our data indicate that 9-phenanthrol inhibits TMEM16A currents at concentrations similar to other second-generation inhibitors. 9-Phenanthrol inhibition of TMEM16A currents exhibited voltage-dependence at higher concentrations, although there were slight differences in the voltage sensitivity of arterial myocyte and recombinant TMEM16A currents. Arterial myocyte current inhibition was voltage-dependent at concentrations ≥15 µM, whereas rTMEM16A currents exhibited voltage-dependent inhibition at lower concentrations. Rat arterial myocyte TMEM16A and the human rTMEM16A clone also generated currents with slightly different rectification when measured using 1 µM free intracellular Ca^{2+} concentration. Explanations for slightly different rectification and voltage sensitivity to 9-phenanthrol include species of the endogenous (rat) and rTMEM16A (human) channels studied, TMEM16A splice variation, and the native cells and recombinant expression systems used. Sequence alignment indicates that full-length rat and human TMEM16A channels are 87% identical. Similarly, TMEM16A channels undergo alternative splicing that can modulate properties, including Ca^{2+}- and voltage-dependence, and this may occur in a cell-type specific manner (Caputo *et al.*, 2008; Ferrera *et al.*, 2009). TMEM16A channels have not been cloned from rat arterial myocytes, and therefore splice variants expressed in this cell type are unclear. Other explanations for slightly different current properties include that HEK293 cells may express an endogenous factor not present in rat arterial myocytes that causes current rectification.

To test the hypothesis that 9-phenanthrol is a non-selective Cl^- channel blocker, we studied bestrophin, another Ca^{2+}-activated Cl^- channel (Sun *et al.*, 2002). Multiple different bestrophin isoforms (1, 2 and 3) are expressed in cultured basilar artery myocytes, A7r5 cells, whole mesenteric arteries and aorta (Wang *et al.*, 2012). It is controversial whether bestrophin-3 can generate an ionic current (Milenkovic *et al.*, 2008). Therefore, we examined 9-phenanthrol regulation of

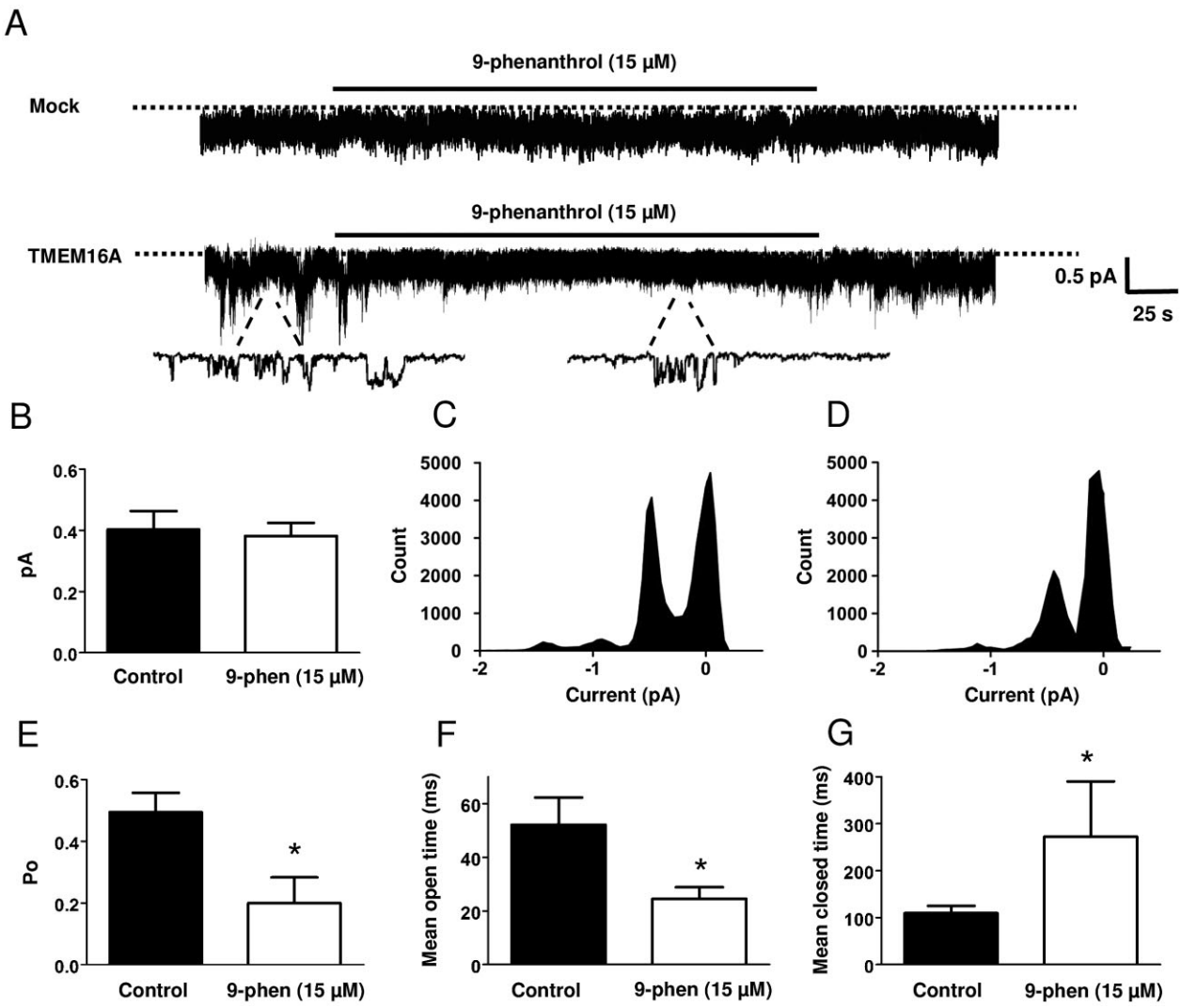

Figure 5

9-Phenanthrol reduces single recombinant TMEM16A channel open probability and open time and elevates mean closed time in HEK293 cells. (A) Original recordings of mock HEK293 cells and single recombinant TMEM16A channels and inhibition by 9-phenanthrol at –80 mV. Traces were filtered at 2 kHz. Single channel amplitude (B), amplitude histograms for control (C) and 9-phenanthrol (D), open probability (P_o) (E), open time (F) and closed time (G) for control (n = 11) and in the presence of 9-phenanthrol (n = 7). *Indicates $P < 0.05$.

bestrophin-1, which generates large membrane currents in HEK293 cells (Fischmeister and Hartzell, 2005). 9-Phenanthrol did not alter bestrophin-1 currents, indicating that 9-phenanthrol displays specificity for TMEM16A Ca^{2+}-activated Cl^- channels.

E_{act} activates TMEM16A channels via a direct mechanism that does not require the presence of intracellular Ca^{2+} (Namkung *et al.*, 2011). E_{act} activated TMEM16A currents in A253 cells, a human submandibular cell line, and in Fisher rat thyroid cells stably expressing TMEM16A channels (Namkung *et al.*, 2011). E_{act} also contracted mouse intestine smooth muscle and stimulated submucosal gland secretion in human bronchi (Namkung *et al.*, 2011). To our knowledge, our data are the first to show that E_{act} stimulates TMEM16A currents in smooth muscle cells. F_{act}, a TMEM16A channel potentiator, stimulates Cl_{Ca} currents in rabbit pulmonary artery smooth muscle cells (Davis *et al.*, 2013). Our data suggest that 9-phenanthrol does not inhibit TMEM16A channels by interfering with the Ca^{2+} activation mechanism. E_{act} stimulated larger currents than we have previously observed to be activated by intracellular Ca^{2+} or cell swelling in cerebral artery myocytes (Bulley *et al.*, 2012). These data suggest that a large residual population of TMEM16A exists in vascular myocytes that can be activated by this agonist. Here, 9-phenanthrol blocked both intracellular Ca^{2+}- and E_{act}-activated TMEM16A currents at similar concentrations in arterial myocytes. Davis *et al.* compared relaxation induced by niflumic acid, tannic acid and $T16A_{inh}$-A01 in thoracic aorta determining that $T16A_{inh}$-A01 was the most potent agent with an apparent IC_{50} of 1.7 μM (Davis *et al.*, 2013). These suggest that $T16A_{inh}$-A01 is an order of magnitude more potent than 9-phenanthrol as a TMEM16A channel

blocker. However, $T16A_{inh}$-A01 specificity is unclear and the experimental preparations used to determine IC_{50}s for 9-phenanthrol (patch clamp) and $T16A_{inh}$-A01 (functional contractility) were different.

There are few published recordings of single TMEM16A channels in the literature. Those reported by other groups were done in excised patches, which produce less seal noise than the whole-cell measurements performed here. Yang *et al.* (2008) did inside-out patch recording in HEK cells and Davis *et al.* (2013) performed outside-out recordings in rabbit pulmonary artery and mouse aortic smooth muscle cells. Our recordings look similar to those of Davis *et al.* (2013). Our data indicate that mock-transfected cells exhibit far less activity when compared with cells overexpressing recombinant TMEM16A. In addition, 9-phenanthrol had no effect on current in mock-transfected cells. These data indicate that 9-phenanthrol inhibits both recombinant and arterial myocyte TMEM16A channels.

9-phenanthrol abolished pressure-induced membrane depolarization and myogenic tone in cerebral arteries (Gonzales *et al.*, 2010). Concentration–response curves generated from these experiments revealed an IC_{50} of 11.4 μM, which was similar to the IC_{50} for TRPM4 current inhibition (IC_{50}, 10.6 μM) in cerebral artery myocytes (Gonzales *et al.*, 2010). From these data, the authors suggested that TRPM4 activation is essential for myogenic constriction (Gonzales *et al.*, 2010). We have recently demonstrated that TMEM16A activation contributes to pressure-induced depolarization and myogenic constriction in rat cerebral arteries (Bulley *et al.*, 2012). Two possibilities existed based on these collective observations: that TRPM4 activation occurs upstream or downstream of TMEM16A activation, or that 9-phenanthrol blocks both TRPM4 and TMEM16A channels to attenuate pressure-induced depolarization. Our data suggest that 9-phenanthrol inhibits myogenic tone by blocking both TMEM16A and TRPM4 channels in cerebral artery smooth muscle cells. This conclusion is supported by data indicating that TMEM16A and TRPM4 currents are sensitive to similar concentrations of 9-phenanthrol and that 9-phenanthrol abolishes myogenic tone at concentrations that block both of these channels (Gonzales *et al.*, 2010).

In summary, we identified 9-phenanthrol as a novel inhibitor of both cerebral artery myocyte and recombinant TMEM16A (rTMEM16A) channels. 9-Phenanthrol reduces TMEM16A channel open probability by lowering mean open time and increasing mean closed time. These data not only identify 9-phenanthrol as a novel TMEM16A channel blocker, but also explain the observation that this molecule abolishes myogenic tone when both TRPM4 and TMEM16A channels contribute to this response. 9-Phenanthrol may be a promising candidate from which to develop TMEM16A channel-specific inhibitors.

Acknowledgements

We thank Drs John Bannister and Dennis Leo for helpful comments on the manuscript. This work was supported by NHLBI/NIH grants (HL110347, HL67061, HL094378) to J. H. J.

Author Contributions

S. K. B. contributed to the conception of the work, data acquisition, data analysis and interpretation of the findings as well as to the drafting and critical revision of the paper. Q. W. contributed to data acquisition and analysis as well as to the critical revision of the paper. S. B. contributed to the conception of the work as well as to the drafting and critical revision of the paper. Z. P. N. contributed to the conception of the work and the critical revision of the paper. J. H. J. contributed to the conception of the work as well as to the drafting and critical revision of the paper.

Conflict of interest

None to report.

References

Alexander SPH, Benson HE, Faccenda E, Pawson AJ, Sharman JL, Spedding M *et al.* (2013). The Concise Guide to PHARMACOLOGY 2013/14: Ion channels. Br J Pharmacol 170: 1607–1651.

Amarouch MY, Syam N, Abriel H (2013). Biochemical, single-channel, whole-cell patch clamp, and pharmacological analyses of endogenous TRPM4 channels in HEK293 cells. Neurosci Lett 541: 105–110.

Brayden JE, Earley S, Nelson MT, Reading S (2008). Transient receptor potential (Trp) channels, vascular tone and autoregulation of cerebral blood flow. Clin Exp Pharmacol Physiol 35: 1116–1120.

Bulley S, Neeb ZP, Burris SK, Bannister JP, Thomas-Gatewood CM, Jangsangthong W *et al.* (2012). TMEM16A/ANO1 channels contribute to the myogenic response in cerebral arteries. Circ Res 111: 1027–1036.

Caputo A, Caci E, Ferrara L, Pedemonte N, Barsanti C, Sondo E *et al.* (2008). TMEM16A, a membrane protein associated with calcium-dependent chloride activity. Science 322: 590–594.

Davis AJ, Shi J, Pritchard HA, Chadha PS, Leblanc N, Vasilikostas G *et al.* (2013). Potent vasorelaxant activity of the TMEM16A inhibitor $T16A_{inh}$-A01. Br J Pharmacol 168: 773–784.

Dietrich A, Mederos YS, Gollasch M, Gross V, Storch U, Dubrovska G *et al.* (2005). Increased vascular smooth muscle contractility in TRPC6-/- mice. Mol Cell Biol 25: 6980–6989.

Earley S, Brayden JE (2010). Transient receptor potential channels and vascular function. Clin Sci (Lond) 119: 19–36.

Earley S, Waldron BJ, Brayden JE (2004). Critical role for transient receptor potential channel TRPM4 in myogenic constriction of cerebral arteries. Circ Res 95: 922–929.

Earley S, Straub SV, Brayden JE (2007). Protein kinase C regulates vascular myogenic tone through activation of TRPM4. Am J Physiol Heart Circ Physiol 292: H2613–H2622.

Ferrera L, Caputo A, Ubby I, Bussani E, Zegarra-Moran O, Ravazzolo R *et al.* (2009). Regulation of TMEM16A chloride channel properties by alternative splicing. J Biol Chem 294: 33360–33368.

Fischmeister R, Hartzell HC (2005). Volume sensitivity of the bestrophin family of chloride channels. J Physiol 562: 477–491.

Gonzales AL, Earley S (2012). Endogenous cytosolic Ca^{2+} buffering is necessary for TRPM4 activity in cerebral artery smooth muscle cells. Cell Calcium 51: 82–93.

Gonzales AL, Garcia ZI, Amberg GC, Earley S (2010). Pharmacological inhibition of TRPM4 hyperpolarizes vascular smooth muscle. Am J Physiol Cell Physiol 299: C1195–C1202.

Grand T, Demion M, Norez C, Mettey Y, Launay P, Becq F *et al.* (2008). 9-phenanthrol inhibits human TRPM4 but not TRPM5 cationic channels. Br J Pharmacol 153: 1697–1705.

Guibert C, Ducret T, Savineau JP (2011). Expression and physiological roles of TRP channels in smooth muscle cells. Adv Exp Med Biol 704: 687–706.

Hill MA, Zou H, Potocnik SJ, Meininger GA, Davis MJ (2001). Invited review: arteriolar smooth muscle mechanotransduction: Ca^{2+} signaling pathways underlying myogenic reactivity. J Appl Physiol 91: 973–983.

Huang F, Zhang H, Wu M, Yang H, Kudo M, Peters CJ *et al.* (2012). Calcium-activated chloride channel TMEM16A modulates mucin secretion and airway smooth muscle contraction. Proc Natl Acad Sci U S A 109: 16354–16359.

Jackson WF (2000). Ion channels and vascular tone. Hypertension 35: 173–178.

Jaggar JH (2001). Intravascular pressure regulates local and global Ca^{2+} signaling in cerebral artery smooth muscle cells. Am J Physiol 281: C439–C448.

Kilkenny C, Browne W, Cuthill IC, Emerson M, Altman DG (2010). Animal research: Reporting in vivo experiments: the ARRIVE guidelines. Br J Pharmacol 160: 1577–1579.

Kim BJ, Nam JH, Kim SJ (2011). Effects of transient receptor potential channel blockers on pacemaker activity in interstitial cells of Cajal from mouse small intestine. Mol Cells 32: 153–160.

Launay P, Cheng H, Srivatsan S, Penner R, Fleig A, Kinet JP (2004). TRPM4 regulates calcium oscillations after T cell activation. Science 306: 1374–1377.

Mazzone A, Eisenman ST, Strege PR, Yao Z, Ordog T, Gibbons SJ *et al.* (2012). Inhibition of cell proliferation by a selective inhibitor of the Ca^{2+}-activated Cl^- channel, Ano1. Biochem Biophys Res Commun 427: 248–253.

McGrath J, Drummond G, McLachlan E, Kilkenny C, Wainwright C (2010). Guidelines for reporting experiments involving animals: the ARRIVE guidelines. Br J Pharmacol 160: 1573–1576.

Meininger GA, Davis MJ (1992). Cellular mechanisms involved in the vascular myogenic response. Am J Physiol 263: H647–H659.

Milenkovic VM, Langmann T, Schreiber R, Kunzelmann K, Weber BH (2008). Molecular evolution and functional divergence of the bestrophin protein family. BMC Evol Biol 8: 72.

Namkung W, Yao Z, Finkbeiner WE, Verkman AS (2011). Small-molecule activators of TMEM16A, a calcium-activated chloride channel, stimulate epithelial chloride secretion and intestinal contraction. FASEB J 25: 4048–4062.

Narayanan D, Bulley S, Leo MD, Burris SK, Gabrick KS, Boop FA *et al.* (2013). Smooth muscle cell transient receptor potential polycystin-2 (TRPP2) channels contribute to the myogenic response in cerebral arteries. J Physiol 591: 5031–5046.

Nelson MT, Patlak JB, Worley JF, Standen NB (1990). Calcium channels, potassium channels, and voltage dependence of arterial smooth muscle tone. Am J Physiol 259: C3–C18.

Nilius B, Prenen J, Janssens A, Voets T, Droogmans G (2004). Decavanadate modulates gating of TRPM4 cation channels. J Physiol 560: 753–765.

Nilius B, Mahieu F, Prenen J, Janssens A, Owsianik G, Vennekens R *et al.* (2006). The Ca^{2+}-activated cation channel TRPM4 is regulated by phosphatidylinositol 4,5-biphosphate. EMBO J 25: 467–478.

Pawson AJ, Sharman JL, Benson HE, Faccenda E, Alexander SP, Buneman OP *et al.*; NC-IUPHAR (2014). The IUPHAR/BPS Guide to PHARMACOLOGY: an expert-driven knowledgebase of drug targets and their ligands. Nucl Acids Res 42 (Database Issue): D1098–D1106.

Schroeder BC, Cheng T, Jan YN, Jan LY (2008). Expression cloning of TMEM16A as a calcium-activated chloride channel subunit. Cell 134: 1019–1029.

Sun H, Tsunenari T, Yau KW, Nathans J (2002). The vitelliform macular dystrophy protein defines a new family of chloride channels. Proc Natl Acad Sci U S A 99: 4008–4013.

Thomas-Gatewood C, Neeb ZP, Bulley S, Adebiyi A, Bannister JP, Leo MD *et al.* (2011). TMEM16A channels generate Ca^{2+}-activated Cl^- currents in cerebral artery smooth muscle cells. Am J Physiol Heart Circ Physiol 301: H1819–H1827.

Wang M, Yang H, Zheng LY, Zhang Z, Tang YB, Wang GL *et al.* (2012). Downregulation of TMEM16A calcium-activated chloride channel contributes to cerebrovascular remodeling during hypertension by promoting basilar smooth muscle cell proliferation. Circulation 125: 697–707.

Yang YD, Cho H, Koo JY, Tak MH, Cho Y, Shim WS *et al.* (2008). TMEM16A confers receptor-activated calcium-dependent chloride conductance. Nature 455: 1210–1215.

Supporting information

Additional Supporting Information may be found in the online version of this article at the publisher's web-site:

http://dx.doi.org/10.1111/bph.13077

Figure S1 9-Phenanthrol inhibits TMEM16A currents in cerebral artery smooth muscle cells when using a pipette free Ca^{2+} concentration of 600 nM. (A) Examples of whole-cell, time-dependent, outwardly rectifying TMEM16A currents recorded in the absence (control) and presence of 9-phenanthrol (10 μM) when using a pipette free Ca^{2+} concentration of 600 nM. (B) Mean data. $n = 7$ each for control and 9-phenanthrol.

Figure S2 Single channel amplitude histogram for a mock-transfected HEK293 cell for control and 9-phenanthrol.